

Urban flood vulnerability assessment of Vadodara city using rainfall–run-off simulations

Harsh D. Patel¹, Gaurav V. Jain^{2,*} and Suvarna D. Shah³

¹S. S. Agrawal Institute of Engineering and Technology, Navsari 396 445, India

²Space Applications Centre, Indian Space Research Organisation, Ahmedabad 380 015, India

³Civil Engineering Department, Faculty of Technology and Engineering, The M. S. University of Baroda, Vadodara 390 001, India

In this study, we demonstrate an approach for citywide urban flood vulnerability assessment based on the capability of storm-water drainage networks. The daily rainfall data of 45 years were used to generate intensity–duration–frequency curves of 2, 5, 10, 50 and 100-yr return periods. The performance of the storm-water drainage network was subsequently evaluated for each of these probable storms using rainfall–run-off simulations employing the SWMM software of US EPA. The duration of flooding at drainage nodes under storms of different return periods was considered for identifying flood-prone regions in the study city. It was observed that about 21% of the city is currently under high and very high urban flood severity zones.

Keywords: Rainfall, return period, run-off, storm-water drainage, urban flood vulnerability.

FLOODS in urban areas are more devastating than in rural areas due to the higher concentration of population and economic activities. While cities may be flooded due to overflowing rivers^{1,2}, sea-level rise^{3,4} and increased groundwater level⁴, severe rainfall exceeding the capacity of the storm-water drainage network is one of the most common and recurring causes of urban floods^{5–7}. In recent years, rapid urbanization has added tremendous pressure on the aging and poorly maintained storm-water drainage infrastructure of cities, resulting in an increase in the incidence of urban floods^{8–10}. Therefore, identifying areas vulnerable to urban floods is essential for timely actions aimed at augmenting the drainage infrastructure and managing such floods effectively.

The vulnerability to urban floods has physical, social and institutional dimensions^{11–13}. The physical vulnerability, defined by the degree of exposure and the capability of the exposed elements to withstand the impact of floods, remains the most studied aspect of urban flood vulnerability assessment¹³. Multi-criteria decision-making techniques in the geographic information system (GIS) environment effectively address the complexity and challenges involved in

flood vulnerability assessment. These techniques have been widely applied for regional-level analysis^{14–17}. Studies have also applied these techniques in the urban environment for flood vulnerability assessment, with city-specific variables^{11,18–20}. Terrain parameters^{18–22}, land use/land cover^{18,20,23} and demographic profile^{11,19,20} are the most commonly used attributes in GIS-based urban flood vulnerability assessment.

The vulnerability to floods in urban areas is managed by providing a storm-water drainage network and other flood protection measures. Therefore, it is desirable to include these infrastructural elements in assessing urban flood vulnerability. Sowmya *et al.*¹⁹ included the density of distance from drainage block sites in assessing urban flood vulnerability. However, estimation of the capacity of the storm-water drainage network in draining out the excess run-off requires the application of mathematical models implementing a 1-dimensional (1D) shallow water wave equation, also referred to as the Saint Venant's equation, considering the non-uniform unsteady flow in drainage networks^{6,24,25}. Dynamic rainfall–run-off models for urban areas, such as the storm-water management model (SWMM) and MIKE-URBAN, integrate the hydrological response of urban catchment with the hydraulics of the underlying drainage network to simulate the flow of run-off^{7,24}. SWMM, developed by Environment Protection Agency (EPA), USA, has been widely used for simulating the response of drainage networks to probable rainfall of longer return periods^{25–27}, climate change impacts^{8,26,28,29} and increased urbanization level⁸. Similarly, MIKE-URBAN and MIKE-FLOOD models have been used for urban flood risk analysis³⁰ and urban flood simulations³¹. These models, however, require detailed information characterizing urban catchment and storm-water drainage networks⁶. The data requirements, simulation efforts and acceptable accuracy of results determine the suitability and applicability of such models³². The digital elevation model (DEM) is an important input for delineating sub-catchments within urban areas besides estimating their slope. While the very high-resolution DEM, typically acquired by LIDAR with better than 1 m resolution, is desirable for modelling urban floods^{27,33}, researchers have utilized 10–30 m resolution DEM for such studies as well^{6,8,26,29}.

*For correspondence. (e-mail: gvj@sac.isro.gov.in)

Similarly, impervious surface cover may be estimated from multiple sources, such as remote sensing images^{6,26} and land-use/land-cover maps²⁹. The scale and spatial resolution often limit the application of urban flood simulation models to smaller regions³⁴. The flood depth and duration of flooding as derived from simulations under storms of varying return periods or changing climatic conditions contribute to urban flood vulnerability assessment in conjunction with socio-economic data^{28,29}. It is therefore evident that while using dynamic rainfall-run-off models over large cities for assessing urban flood vulnerability is desirable, its application shows wide variability owing to the availability of data for model parameterization.

Cities are expanding at an unprecedented pace, particularly in developing countries. In India, although the share of urban population in total population accounted for merely 31.28% in 2011 (ref. 35), the urban population in absolute numbers increased by 31.8% over that of the year 2021. IPCC³⁶ noted that increased urbanization could intensify extreme rainfall and run-off intensities in the future. The ClimateSMART Cities Assessment Framework, devised by the Government of India (GoI), also recommends cities to prepare flood-risk assessment plans and address future flood risks³⁷. Considering the frequent occurrence of urban floods in Indian cities and possible climate-induced changes in precipitation rates in the future, this study demonstrates an approach for citywide urban flood vulnerability assessment based on the capability of storm-water drainage networks. The study proposes a drainage network-driven approach to model urban storm-water flows in Vadodara city, Gujarat, India.

Study area

Vadodara is situated along the banks of Vishwamitri River, which is further joined by Jambuva River in the southern

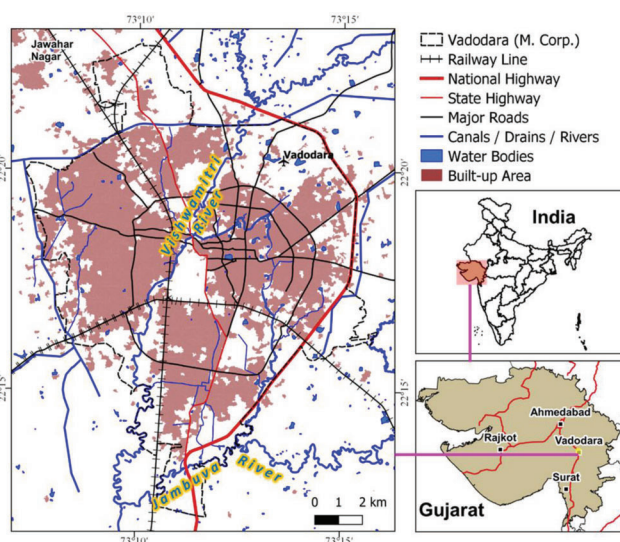


Figure 1. Map showing Vadodara Municipal Corporation, Gujarat, India.

part of the city (Figure 1). It is the third largest city in Gujarat, after Ahmedabad and Surat. Vadodara is also one of the six cities from Gujarat which are included in the Smart Cities Mission of GoI. The city is governed by the Vadodara Municipal Corporation (VMC). The population of VMC increased from 1,338,244 in 2001 to 1,670,806 in 2011, thereby growing at the rate of 2.24% per annum. At this rate, the population of the city is likely to exceed 2.5 million by 2031.

Vadodara has an underground storm-water drainage network comprising conduits of circular and closed-rectangular cross-sections. This drainage network was constructed in phases over several years, as in the case of most Indian cities. The storm-water drainage network of Vadodara was upgraded to provide 100% coverage to the developed area of the city by December 2012 (ref. 38). The inadequate maintenance and desilting of the drainage network, along with delays in its upgradation and augmentation have resulted into frequent waterlogging in several parts of the city during monsoon season³⁹. The sub-surface drainage network of Vadodara is also supported by the network of open channels, called *kaans* in the local language, draining into the rivers. The encroachment of these open channels by uncontrolled urbanization has resulted in their change in alignment and gradient at several places³⁹. Similarly, the unplanned and haphazard development, coupled with the encroachment of riverbed, has significantly narrowed the Vishwamitri River in several places.

Urban floods have become a recurrent problem for Vadodara city, primarily on account of heavy rainfall that exceeds the capacity of the drainage network to remove excess run-off. Incidents of very heavy rainfall (amount realized in a day was between 124.5 and 244.4 mm) and extremely heavy rainfall (amount realized in a day was more than or equal to 244.4 mm) have increased substantially over the past few years (Figure 2). Vadodara experienced severe floods in 2005 when it received exceptionally heavy rainfall of over 315 mm daily. In 2019, the city again witnessed exceptionally heavy rainfall of 442 mm in just 12-h period, causing widespread devastation⁴⁰. While the drainage network now covers most of the city's built-up areas³⁸, the unchecked urban expansion coupled with heavy rainfall has increased its vulnerability to urban floods.

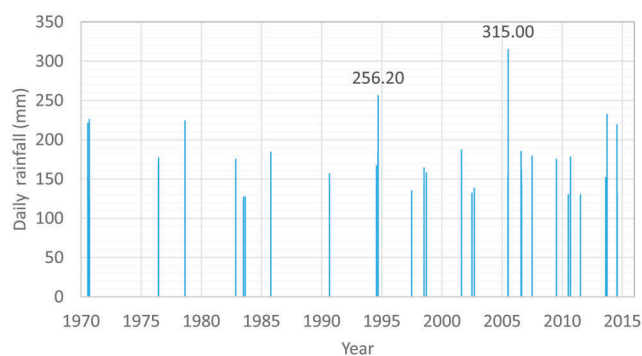


Figure 2. Very heavy and extremely heavy rainfall in Vadodara.

Methodology

IRS Resourcesat-2 LISS-IV data with 5.8 m spatial resolution, acquired on 18 October 2014, was used for mapping land use/land cover and estimating impervious surface cover in the study area. The digital elevation model (DEM) and digital terrain model (DTM) of the study area were generated using the Cartosat-1 stereo pair acquired on 7 December 2014. Daily rainfall data from 1970 to 2015 were collected from the State Water Data Centre (SWDC), Gandhinagar. The storm-water drainage network of Vadodara was obtained from the Drainage Department of VMC. Soil texture information was also obtained from VMC.

Generation of rainfall time series

The daily rainfall data were converted into hourly rainfall data using the following empirical equation²⁶:

$$P_t = P_{24} \sqrt[3]{\frac{t}{24}}, \quad (1)$$

where P_t is the rainfall depth (mm) corresponding to duration t (h), P_{24} the daily rainfall depth (mm) and t is the duration of rainfall (h). Maximum daily rainfall of each year from 1970 to 2015 was used for P_{24} . The hourly rainfall (rainfall intensity) of various durations like 1 h, 2 h, 6 h, 12 h and 24 h were calculated from these annual maximum values. The mean and standard deviation of rainfall intensity for different durations were estimated. Gumbel's extreme value distribution was applied for generating the intensity–duration–frequency (IDF) curves. The rainfall intensity at a given return period is given by eq. (2).

$$X_T = \bar{X} + K_T S, \quad (2)$$

where X_T is the rainfall intensity at a given return period, \bar{X} the mean rainfall intensity of a particular duration t , S the standard deviation of rainfall intensity and K_T is the frequency factor. The frequency factor for different return periods were computed using eqs (3) and (4), and further adjusted for the sample size of 45-year rainfall data with reduced mean and reduced standard deviation⁴¹.

$$Y_T = - \left[\ln \left(\ln \frac{T}{T-1} \right) \right], \quad (3)$$

$$K_T = \frac{Y_T - 0.577}{1.2825}. \quad (4)$$

The IDF curves were thus generated for 2-, 5-, 10-, 50- and 100-yr return periods. These IDF curves were used for generating rainfall time-series of 24 h duration, such that rainfall depth from 0 to t h duration corresponded to the total rainfall depth derived from the IDF curves.

Data preparation for SWMM

The storm-water pipelines were delineated from the maps in PDF files obtained from VMC as linear features. These linear features were transformed into a directed graph network with link-node topology. The properties of conduits, such as their origin and destination nodes, dimensions, shape, Manning's coefficient and slope, were assigned from these files. Similarly, invert levels at junctions and outfalls were assigned from the ancillary data. The storm-water drainage network of the study area was thus prepared.

The built-up area was extracted from IRS Resourcesat-2 LISS-4 image using a two-stage, object-based nearest neighbor classification approach with hierarchical segmentation⁴². The built-up area thus classified was corrected using visual interpretation in a GIS environment for better accuracy. Figure 1 shows the built-up area distribution in the study area. Maximum likelihood classification was subsequently applied in the remaining area for land-use/land-cover classification. Cartosat-1 stereo pair comprising fore and aft images was used to generate DEM with 157 ground control points (GCPs) collected by Shah⁴³. The elevation points in open spaces were interpolated to generate DTM at 5 m spatial resolution.

DTM can be used for deriving sub-catchment areas and drainage networks. However, in densely built regions of the study area, open spaces are scarce and therefore extraction of DTM is difficult. The sub-catchment areas were, therefore, derived from the storm-water drainage network. Theissen polygons of storm-water drainage network nodes were used as sub-catchment areas, with each node acting as the outlet of the respective sub-catchment. The proportion of impervious surface cover was derived by integrating sub-catchment areas with the built-up area. Manning's coefficient for pervious and impervious surfaces was assumed from SWMM typical values based on dominant land use/land cover within the sub-catchment⁴⁴ (Table 1). The depression storage of 5.0 and 2.5 mm was assumed over pervious and impervious surfaces respectively⁴⁴. Soil properties for Curve number method were assigned to each sub-catchment based on soil texture. The analysis of rainfall records of 45 years indicated average antecedent dry days during the monsoon period (July–September) as 3.8. In the present study, however, antecedent dry days were set to zero for a worst-case scenario. Mean slope was estimated from DTM. Characteristic width was approximated as the

Table 1. Manning's coefficient on pervious and impervious surfaces

Type of surface	Land cover/land use	Manning's coefficient
Impervious surface	Built-up area	0.012
	Roads	0.011
Pervious surface	Cropland	0.170
	Recreational (parks, etc.)	0.150
	Fallow land	0.050
	Vacant land	0.050

ratio of the average distance between all feature vertices of the sub-catchment and the area of the sub-catchment.

The data of sub-catchments, conduits, junctions and outfalls were converted to SWMM input file using the conversion tool developed by Jain *et al.*⁶. The input file, thus generated, comprises sub-catchments, conduits, junction nodes and outfall nodes. The rainfall time series along with the rain gauge were added after opening the input file in SWMM software.

Urban flood vulnerability assessment

The rainfall time series derived from IDF curves were assigned to the rain gauge in SWMM. The simulation was performed for rainfall time series corresponding to 2-yr, 5-yr, 10-yr, 50-yr and 100-yr return periods to obtain the estimated duration of node flooding. SWMM treats a sub-catchment area as a nonlinear reservoir and computes the overland run-off (Q , m³/s) due to rainfall excess using Manning’s equation (eq. (5))⁴⁴. The inflow to a sub-catchment area is from precipitation, as provided by the rainfall time series, while the outflow is in the form of evaporation, depression storage, infiltration and surface run-off. The overland flow occurs only when the depth of water (d) in a sub-catchment exceeds the maximum depression storage (d_p)⁶.

$$Q = \frac{W}{n} (d - d_p)^{5/3} S^{1/2}, \tag{5}$$

where W is the characteristic width (m), n the Manning’s coefficient of roughness and S is the sub-catchment slope.

The storm-water flow in the drainage network was modeled as 1D gradually varying unsteady flow represented by Saint Venant’s equations⁴⁴. These equations are approximations of the momentum and continuity equations given below.

Continuity equation:

$$\frac{\partial y}{\partial t} + \frac{\partial(uy)}{\partial x} = q. \tag{6}$$

Momentum equation:

$$\frac{1}{g} \frac{\partial u}{\partial t} + \frac{u}{g} \frac{\partial u}{\partial x} + \frac{\partial y}{\partial x} = S_0 - S_f - \frac{q}{g} \frac{u}{y}, \tag{7}$$

where u is the flow velocity, y the water depth, x the distance, t the time, q the lateral inflow per unit length perpendicular to the channel, g the acceleration due to gravity, S_0 the bed slope and S_f is the friction slope. These differential equations of flow were solved by SWMM using finite difference method.

The flood risk was assigned to the sub-catchments based on the duration of flooding at their outlet node for storms corresponding to all return periods. The flood-risk score was assigned based on the duration of flooding for storms

of each return period (Table 2), and the total score for all the selected return periods was computed. The final score was similarly classified according to Table 2 to assign urban flood risk.

The urban flood risk thus derived was integrated with population density to assess urban flood vulnerability. The ward-level population corresponding to the years 2001 and 2011 was obtained from the Primary Census Abstracts (PCA) published by the Census of India^{35,45}. The population of each ward was projected for the year 2014 using the geometric increase method. The ratio of the estimated population of 2014 and the built-up area provided the net population density of 2014 for each ward. The flood severity (as defined by the duration of floods due to storms of different return periods) with population density was used to determine urban flood vulnerability.

Results and discussion

The historical rainfall data were used to estimate probable rainfall time series for 2-yr, 5-yr, 10-yr, 50-yr and 100-yr return periods. These were used for estimating the duration of flooding in the storm-water drainage network, which was subsequently integrated with demographic characteristics of the sub-catchment areas to assess urban flood vulnerability in Vadodara.

IDF curves and rainfall time series

Figure 3 shows the IDF curves derived from daily rainfall data of 45 years. The probable maximum daily rainfall for Vadodara city corresponding to 2-yr, 5-yr, 10-yr, 50-yr and 100-yr return periods was 124.37, 183.44, 222.20, 307.91 and 344.16 mm respectively, whereas the corresponding maximum rainfall rate was 43.12, 63.59, 77.03, 106.75 and 119.32 mm/h respectively. The daily rainfall corresponding to 50-yr and 100-yr return periods was classified as extremely heavy rainfall (daily rainfall greater than 244.4 mm) whereas that of 2-yr, 5-yr and 10-yr return periods was categorized as very heavy rainfall (daily rainfall more than 124.5 and less than 244.4 mm), according to the classification by India Meteorological Department. The storm-water drainage networks in India are typically designed for a rainfall rate corresponding to a 1-yr return period for dense residential areas, whereas a rainfall rate

Table 2. Definition of flood risk zones

Duration of flooding (h)	Flood risk	Score	Final score
0–6	Very low risk	1	1–5
6–12	Low risk	2	6–10
12–18	Moderate risk	3	11–15
18–24	High risk	4	16–20
>24	Very high risk	5	20–25

corresponding to a 2-yr return period is recommended for commercial areas⁴⁶. However, considering the increase in rainfall intensities induced by climate change, IDF relationships may need adjustments⁴⁷. The assessment of the response of storm-water drainage networks to rainfall of different return periods can be used to prepare for such exigencies. The time series derived from the 24-h rainfall of different return periods was used as a forcing function in simulating the storm-water drainage network response.

Dynamic simulations in SWMM

The catchment area was sub-divided into 1728 sub-catchments. The drainage network comprises 1750 junction nodes and 156 outfall nodes. The artificial surfaces derived from the remote sensing data covered a 6332.73 ha area (41.93% of the total area) within municipal limits. Figure 4 shows the estimated proportion of impervious surface cover in

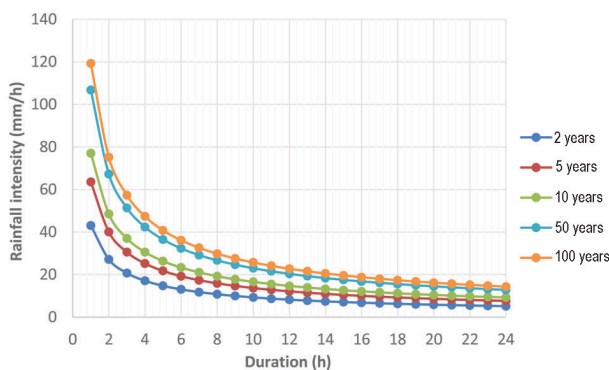


Figure 3. Intensity duration frequency curves.

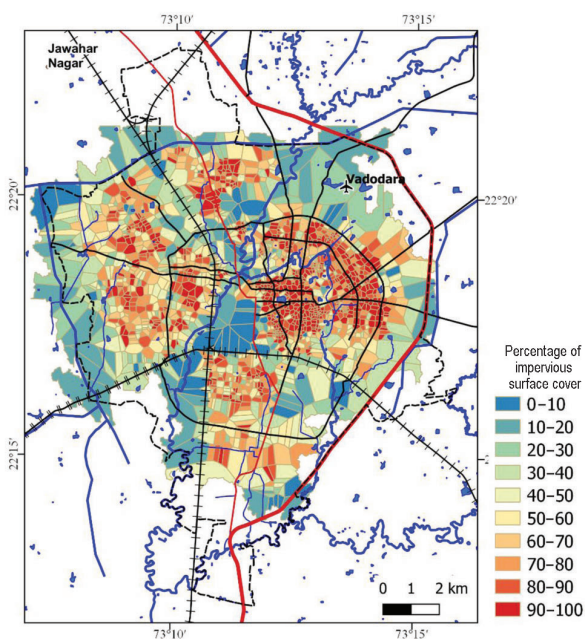


Figure 4. Sub-catchments and impervious surface cover.

each of the sub-catchments. It was observed that 856 sub-catchments had more than 75% impervious surface cover and occupied 2650 ha area of Vadodara. These sub-catchments with high proportion of impervious surface cover are spread in four clusters. The eastern part of Vadodara, which is also the oldest and most densely populated region, was the largest of these clusters (Figure 4). Similar regions with high impervious surface cover are present in the northern, eastern and western parts of the city.

The simulation of storm-water flow in the drainage network under varying precipitation conditions corresponding to design storms of 2-yr, 5-yr, 10-yr, 50-yr and 100-yr return periods was performed using dynamic wave-flow routing in SWMM. It was performed for three days to enable complete evacuation of storm water from the drainage network. Hazen Williams's equation was used to estimate friction losses during pressurized flow conditions in conduits with circular cross-sections. The ponding of excess water at nodes was not modelled in the dynamic wave-flow routing. This prevented excess water from returning into the system as conditions permit. The proportion of precipitation converted to surface run-off varied from 83.4% for the 2-yr return period to 94.39% for the 100-yr return period rainfall time series. The surface run-off thus generated enters the storm-water drainage network as wet weather inflow and is eventually drained out as external outflow, whereas the excess run-off overflows as flooding loss. The flooding loss in rainfall time series corresponding to a 2-yr return period was estimated at 43.13%, whereas that for a 100-yr return period was 65.28%. The run-off continuity error was less than 2%, whereas flow continuity errors were less than 5%. The continuity errors of less than 5–10% indicate the numerical stability of the solution of the Saint-Venant equations⁴⁴.

The duration of flooding and surcharging at the storm-water drainage network nodes were analysed to assess the impact of storms of different return periods. The nodes are considered to be flooded if water overflows from them⁴⁴. Surcharging refers to the condition when the water level at a node rises above the top of the highest conduit, thereby leading to pressurized flow in the conduits connected at the nodes⁴⁴. The duration of flooding at 72 nodes in the storm-water drainage network exceeded 12 h for the 2-yr return period rainfall time series. Similarly, 114, 146, 227 and 258 nodes were likely to be flooded for over 12 h duration under the influence of probable storms of 5-yr, 10-yr, 50-yr and 100-yr return periods respectively. These nodes are mainly situated in the peripheral areas of Vadodara, primarily on the upstream-end of the storm-water drainage network. While the number of nodes that may be flooded is less than 15% of the total nodes, even for probable storms of a 100-yr return period, the proportion of nodes that are flowing under surcharge for over 12 h varies from 30% (510 nodes) to 60% (1038 nodes) for storms with 2-yr and 100-yr return periods respectively. The area of sub-catchments affected by the nodes flooded for over 12-h duration under the influence of a storm with over 100-yr

return period was estimated as 5815.11 ha, accounting for 43.26% of total area, whereas that for the 2-yr return period storm may affect 2155.24 ha area covering only 16.03% of the total area. Figure 5 shows the duration of floods in sub-catchment areas under storms of different return periods. It is apparent that 10% of sub-catchment areas will be flooded for over 24-h duration under 2-yr return period storms, which will increase to 25% under storms of a 100-yr return period. Therefore, it is apparent that the storm-water drainage network in Vadodara is currently inadequate in completely draining out the surface run-off, and may result in frequent surface inundation and waterlogging in the city. Moreover, rainfall of longer return periods is likely to affect larger areas due to these limitations of the storm-water drainage network, as it is already under surcharge conditions.

Urban flood risk zones

The duration of floods^{26,28}, peak run-off²⁷ and flood inundation depth^{28,29} have been used as indicators of urban flood severity in various simulation-based studies. In the present study, flood duration at the nodes has been used to assess the flood severity of the connected sub-catchment area, as surface ponding was not modelled. The ponded area depends on local topography⁴⁴, which will require high-resolution DTM. As the same was not available in this study, flood duration at the sub-catchment outlet alone was used to define flood severity. The flood duration was divided into 6-h intervals, with areas having flood duration less than 6 h being categorized as low-risk zones and those with greater than 24 h flood duration being very high-risk zones. Flood severity scores for storms of 2-yr, 5-yr, 10-yr, 50-yr and 100-yr return periods were assigned according to the respective flood duration. Subsequently, the summation of the score under storms of different return periods was carried out to assess the risk of urban floods in each sub-catchment

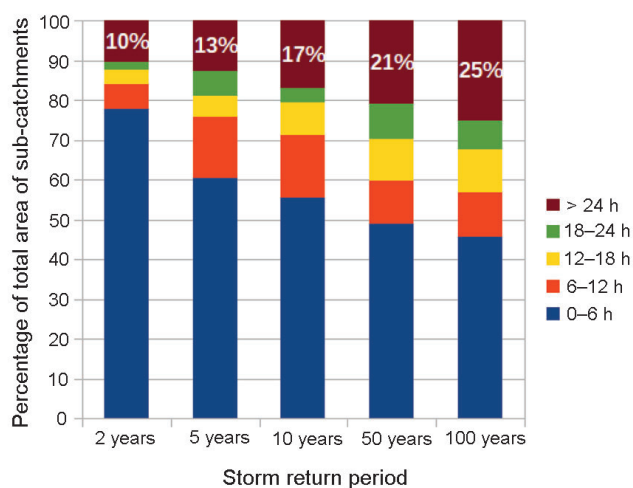


Figure 5. Flood duration in the sub-catchment area under storms of different return periods.

(Table 2). It was observed that about 15% of Vadodara, spread over a 2267 ha land area, is currently under high and very high urban flood risk zones. These are largely situated in the peripheral areas of the city.

The net population density in each sub-catchment area was used to assess the vulnerability to urban floods. The built-up area, as extracted from satellite images, corresponded to the year 2014, whereas the nearest ward-wise population data corresponded to 2011. Thus, the ward-wise population was projected to the year 2014 prior to the computation of net population density. The ward-wise population, as obtained from the Census of India for 2001 (ref. 45) and 2011 (ref. 35), was used to compute the compound annual growth rate (CAGR) of the population, which was subsequently used to estimate the population for the year 2014. The net population density for 2014 was computed as the ratio of an estimated population of 2014 and the built-up area of the same year. The average net population density of wards was 300 persons per hectare (pph). The ward-wise population density and built-up area were used to estimate the ward-wise population density of sub-catchment areas. The net population density and flood severity were cross-tabulated and area statistics were computed (Table 3). The regions with very high severity and very high population density were categorized as very highly vulnerable. As shown in Figure 6, they cover 284.49 ha of land. The high and moderately vulnerable regions cover 1408.24 and 1187.68 ha land areas in Vadodara. Thus, 11.20% of 151 km² of municipal land has very high to high urban flood vulnerability in the city.

Conclusion

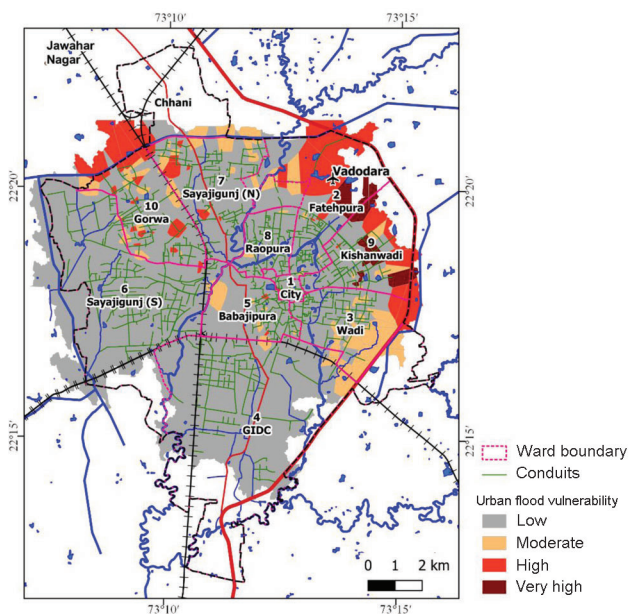
Storm-water drainage network forms an essential part of the strategy to mitigate urban floods. In India, storm-water drainage networks in the larger parts of urban areas are designed for rainfall up to a 2-yr return period only⁴⁶. However, cities are witnessing severe storms at a higher frequency than previously anticipated. IPCC warns of greater risks of extreme weather events, including heavy rainfall in urban areas due to climate change³⁶. The non-availability of necessary data constrains the cities in developing countries such as India from supporting scientific decision-making. NDMA guidelines for the management of urban flooding recommend cities to establish a dense network of automatic rain gauge stations, obtain very high-resolution DEM with 1–2 m contour intervals, and create an inventory of storm-water drainage networks on GIS platform⁴⁷. Much of this information remains elusive to many cities in India. In recent years, projects such as AMRUT and Smart Cities Mission have encouraged cities to generate geospatial data. However, integrating such data with models is an area of concern. The present study has demonstrated the application of SWMM for assessing urban flood vulnerability using data that are commonly available in most Indian cities in conjunction with remote sensing data. The model results can

Table 3. Urban flood vulnerable areas in Vadodara Municipal Corporation, Gujarat, India

Urban flood severity	Net population density (pph)				Total area (ha)
	Low	Moderate	High	Very high	
Very low severity	2,515.97	543.08	2623.53	467.06	6,149.64
Low severity	100.30	138.02	648.54	170.81	1,057.67
Moderate severity	1,077.08	447.38	376.77	63.14	1,964.37
High severity	528.56	97.29	183.30	162.60	971.75
Very high severity	717.69	203.10	1,062.34	284.49	2,267.62
Total area (ha)	4,939.60	1,428.87	4,894.48	1,148.10	

Colour scale: Urban flood vulnerability

Low	Moderate	High	Very high
-----	----------	------	-----------

**Figure 6.** Urban flood vulnerability zones in Vadodara.

further be improved with systematic calibration and validation. The calibration of SWMM requires a reasonably good initial estimate of model parameters, along with reference datasets of run-off volume, peak flow and instantaneous flows to compare and refine the model outcomes⁶. The non-availability of such reference datasets for calibration in this study necessitated use of inference models. These inference models derive the control parameter values using hydrological, hydraulic or other characteristics of the catchment⁴⁸.

Identifying areas vulnerable to urban floods are essential for timely actions aimed at augmenting the infrastructure and managing such floods effectively. It was observed that the storm-water drainage network of Vadodara city might need augmentation in the near future given that almost 30% of its nodes were surcharged for over 12 h duration under the influence of a storm of 2-yr return period. The frequency of very heavy and extremely heavy rainfall has increased drastically in the study area in the past few years. The city witnessed an exceptionally heavy rainfall of over 442 mm in 12 h in 2019 (ref. 40). Therefore, it needs to

prepare for such exigencies in the future as well. We further observed that about 21.45% of the municipal area, spread over 3239 ha land, is currently under high and very high urban flood severity zones, derived based on the response of storm-water drainage networks to storms of 2-yr, 5-yr, 10-yr, 50-yr and 100-yr return periods. Moreover, 52% of this area is currently in rapidly growing and densely populated regions, making it more vulnerable to loss of lives and property. These areas may be prioritized to augment the storm-water drainage network, and alternative techniques such as low-impact development, water-sensitive urban design, sustainable urban drainage systems and green infrastructure may be promoted to build climate resilience into the system⁴⁹. The approach proposed in this study for city-wide urban flood vulnerability assessment based on the capability of the storm-water drainage network can be expanded to other Indian cities to minimize the impact of urban floods while building climate resilience.

1. Patel, D. P. *et al.*, Assessment of flood inundation mapping of Surat city by coupled 1D/2D hydrodynamic modeling: a case application of the new HEC-RAS 5. *Nat. Hazards*, 2017, **89**, 93–130.
2. Tierolf, L. *et al.*, Modeling urban development and its exposure to river flood risk in Southeast Asia. *Comput. Environ. Urban Syst.*, 2021, **87**, 101620; doi:10.1016/j.compenvurbsys.2021.101620.
3. Dutta, D., An integrated tool for assessment of flood vulnerability of coastal cities to sea-level rise and potential socioeconomic impacts: a case study in Bangkok, Thailand. *Hydrol. Sci. J.*, 2011, **56**(5), 805–823.
4. Rotzoll, K. and Fletcher, C. H., Assessment of groundwater inundation as a consequence of sea-level rise. *Nature Climate Change*, 2013, **3**(5), 477–481.
5. Gupta, K., Urban flood resilience planning and management and lessons for the future: a case study of Mumbai, India. *Urban Water J.*, 2007, **4**(3), 183–194.
6. Jain, G. V. *et al.*, Estimation of sub-catchment area parameters for storm water management model (SWMM) using geo-informatics. *Geocarto Int.*, 2016, **21**(4), 462–476.
7. Hammond, M. *et al.*, A new flood risk assessment framework for evaluating the effectiveness of policies to improve urban flood resilience. *Urban Water J.*, 2018, **15**(5), 427–436.
8. Huong, H. T. L. and Pathirana, A., Urbanization and climate change impacts on future urban flooding in Can Tho city, Vietnam. *Hydrol. Earth Syst. Sci.*, 2013, **17**, 379–394.
9. Zope, P. E. *et al.*, Hydrological impacts of land use–land cover change and detention basins on urban flood hazard: a case study of

- Poisar River basin, Mumbai, India. *Nat. Hazards*, 2017, **87**, 1267–1283.
10. Zhou, Q. *et al.*, Impacts of changing drainage indicators on urban flood volumes in historical urbanization in the case of Northern China. *Urban Water J.*, 2021, **18**(7), 487–498; doi:10.1080/15730-62X.2021.1893366.
 11. Muller, A. *et al.*, Assessment of urban vulnerability towards floods using an indicator-based approach – a case study for Santiago de Chile. *Nat. Hazards Earth Syst. Sci.*, 2011, **11**, 2107–2123.
 12. Scheuer, S. *et al.*, Exploring multi-criteria flood vulnerability by integrating economic, social and ecological dimensions of flood risk and coping capacity: from a starting point view towards an end-point view of vulnerability. *Nat. Hazards*, 2011, **58**(2), 731–751.
 13. Cho, S. Y. and Chang, H., Recent research approaches to urban flood vulnerability, 2006–2016. *Nat. Hazards*, 2017, **88**, 633–649.
 14. Lee, G. *et al.*, Integrated multi-criteria flood vulnerability approach using fuzzy TOPSIS and Delphi technique. *Nat. Hazards Earth Syst. Sci.*, 2013, **13**, 1293–1312.
 15. Stefanidis, S. and Stathis, D., Assessment of flood hazard based on natural and anthropogenic factors using analytic hierarchy process (AHP). *Nat. Hazards*, 2013, **68**, 569–585.
 16. Papaioannou, G. *et al.*, Multi-criteria analysis framework for potential flood prone areas mapping. *Water Resour. Manage.*, 2015, **29**, 399–418.
 17. Mukhopadhyaya, A. *et al.*, Characterizing the multi-risk with respect to plausible natural hazards in the Balasore coast, Odisha, India: a multi-criteria analysis (MCA) appraisal. *Nat. Hazards*, 2016, **80**, 1495–1513.
 18. Ouma, Y. O. and Tateishi, R., Urban flood vulnerability and risk mapping using integrated multi-parametric AHP and GIS: methodological overview and case study assessment. *Water*, 2014, **6**, 1515–1545.
 19. Sowmya, K. *et al.*, Urban flood vulnerability zoning of Cochin city, southwest coast of India, using remote sensing and GIS. *Nat. Hazards*, 2015, **75**, 1271–1286.
 20. Sarmah, T. *et al.*, Assessing human vulnerability to urban flood hazard using the analytic hierarchy process and geographic information system. *Int. J. Disast. Risk Reduct.*, 2020, **50**, 101659.
 21. Clement, A. R., An application of geographic information system in mapping flood risk zones in a north central city in Nigeria. *Afr. J. Environ. Sci. Technol.*, 2013, **7**(6), 365–371.
 22. Jalayer F. *et al.*, Probabilistic GIS-based method for delineation of urban flooding risk hotspots. *Nat. Hazards*, 2014, **73**, 975–1001.
 23. Ibarra, E. M., A geographical approach to post-flood analysis: the extreme flood event of 12 October 2007 in Calpe (Spain). *Appl. Geogr.*, 2012, **32**, 490–500.
 24. Zoppou, C., Review of urban storm water models. *Environ. Model. Softw.*, 2001, **16**, 195–231.
 25. Bisht, D. S. *et al.*, Modeling urban floods and drainage using SWMM and MIKE URBAN: a case study. *Nat. Hazards*, 2016, **84**, 749–776.
 26. Andimuthu, R. *et al.*, Performance of urban storm drainage network under changing climate scenarios: flood mitigation in Indian coastal city. *Sci. Rep.*, 2019, **9**, 7783.
 27. Bhattacharjee, S. *et al.*, Hydrodynamic modelling and vulnerability analysis to assess flood risk in a dense Indian city using geospatial techniques. *Nat. Hazards*, 2021, **105**, 2117–2145.
 28. Dasgupta, S. *et al.*, A megacity in a changing climate: the case of Kolkata. *Climate Change*, 2013, **116**, 747–766.
 29. Vemula, S. *et al.*, Urban floods in Hyderabad, India, under present and future rainfall scenarios: a case study. *Nat. Hazards*, 2018, **95**, 637–655.
 30. Ahmad, S. S. and Simonovic, S. P., Spatial and temporal analysis of urban flood risk assessment. *Urban Water J.*, 2013, **10**(1), 26–49.
 31. Le, T. T. A. *et al.*, Urban flood hazard analysis in present and future climate after statistical downscaling: a case study in Ha Tinh city, Vietnam. *Urban Water J.*, 2021, **18**(4), 257–274; doi:10.1080/157-3062X.2021.1877744.
 32. Apel, H. *et al.*, Flood risk analyses – how detailed do we need to be? *Nat. Hazards*, 2009, **49**, 79–98.
 33. Warsta, L. *et al.*, Development and application of an automated sub-catchment generator for SWMM using open data. *Urban Water J.*, 2017, **14**(11), 1–10.
 34. Xing, Y. *et al.*, City scale hydrodynamic modelling of urban flash floods: the issues of scale and resolution. *Nat. Hazards*, 2019, **96**, 473–496.
 35. Census of India, Primary Census Abstracts (Census of India 2011). Office of Registrar General of India, Government of India (GoI), 2011.
 36. Masson-Delmotte, V. *et al.* (eds), *Climate Change 2021: The Physical Science Basis. Contribution of Working Group I to the Sixth Assessment Report of the Intergovernmental Panel on Climate Change*, Cambridge University Press, Cambridge, UK and New York, USA, 2021.
 37. MoHUA, ClimateSMART Cities Assessment Framework, Ministry of Housing and Urban Affairs, GoI, 2019.
 38. VMC, Vadodara Mahanagar Seva Sadan: storm water drainage project. Vadodara Municipal Corporation, Gujarat, 2013; <https://vmc.gov.in/> (accessed on April 2022).
 39. VMC, City development plan. Vadodara Municipal Corporation, Gujarat, 2005.
 40. *Business Standard*, Heavy rainfall throws life out of gear in Vadodara; Airport operations shut. last updated on 1 August 2019; https://www.business-standard.com/article/current-affairs/heavy-rainfall-throws-life-out-of-gear-in-vadodara-airport-operations-shut-119080100330_1.html (accessed in April 2022).
 41. Garg, S. K., *Irrigation Engineering and Hydraulic Structures*, Khanna, Delhi, 1999.
 42. Jain, G. V. and Sharma, S. A., Spatio-temporal analysis of urban growth in selected small, medium and large Indian cities. *Geocarto Int.*, 2019, **34**(8), 887–908.
 43. Shah, S. D., Development of an integrated model for flood management at Vadodara City, M.E. dissertation, S. V. National Institute of Technology, Surat, 2013.
 44. Rossman, L. A., *Report No. EPA/600/R-17/111: Storm Water Management Model Reference Manual, Volume II – Hydraulics*, US Environmental Protection Agency, Cincinnati, OH, USA, 2017.
 45. Census of India, Primary Census Abstracts (Census of India 2001). Office of Registrar General of India, GoI, 2001.
 46. CPHEEO, *Manual on Sewerage and Sewage Treatment, Part-A: Engineering*, Central Public Health and Environmental Engineering Organization, New Delhi, 2013.
 47. NDMA, *National Disaster Management Guidelines Management of Urban Flooding*, National Disaster Management Authority, GoI, 2010.
 48. Choi, K. and Ball, J. E., Parameter estimation for urban runoff modelling. *Urban Water J.*, 2002, **4**, 31–41.
 49. Fletcher, T. D. *et al.*, SUDS, LID, BMPs, WSUD and more – the evolution and application of terminology surrounding urban drainage. *Urban Water J.*, 2015, **12**(7), 525–542.

ACKNOWLEDGEMENTS. We thank the Space Applications Centre (SAC), ISRO, Ahmedabad, for providing the opportunity to carry out work under the Training and Research in Earth Eco-system (TREES) programme at SAC. The support and encouragement provided by Dr I. M. Bahuguna (Deputy Director, EPSA/SAC), Mr Shashikant Sharma (Group Director, VRG/SAC), Mr Hireen Bhatt (Head, CGDD/SAC), Dr Rashmi Sharma (Group Director, AOSG/SAC) and Dr B. Kartikeyan (Head, IAQD/SAC) are deeply acknowledged. We also thank Dr S. P. Vyas (Head, SRTD/SAC) for efficient conduct of the TREES programme.

Received 27 April 2022; revised accepted 5 September 2022

doi: 10.18520/cs/v124/i1/79-86